A four compartment epidemic model with retarded transition rates

Téo Granger, Thomas M Michelitsch, Michael Bestehorn, Alejandro P Riascos, Bernard A Collet

A four compartment epidemic model with retarded transition rates

Téo Granger[1], Thomas M. Michelitsch[1]*, Michael Bestehorn[2],
Alejandro P. Riascos[3], Bernard A. Collet[1]
[1] Sorbonne Université
Institut Jean le Rond d'Alembert CNRS UMR 7190
4 place Jussieu, 75252 Paris cedex 05, France
[2] Brandenburgische Technische Universität Cottbus-Senftenberg
Institut für Physik
Erich-Weinert-Straße 1, 03046 Cottbus, Germany
[3] Instituto de Física, Universidad Nacional Autónoma de México
Apartado Postal 20-364, 01000 Ciudad de México, México

October 18, 2022

Abstract

We study an epidemic model for a constant population by taking into account four compartments of the individuals characterizing their states of health. Each individual is in one of the compartments susceptible (S); incubated – infected yet not infectious (C), infected and infectious (I), and recovered – immune (R). An infection is 'visible' only when an individual is in state I. Upon infection, an individual performs the transition pathway $\mathrm{S} \to \mathrm{C} \to \mathrm{I} \to \mathrm{R} \to \mathrm{S}$ remaining in each compartments C, I, and R for certain random waiting time t_C, t_I, t_R, respectively. The waiting times for each compartment are independent and drawn from specific probability density functions (PDFs) introducing memory into the model. The first part of the paper is devoted to the macroscopic SCIRS model. We derive memory evolution equations involving convolutions (time derivatives of general fractional type). We consider several cases. The memoryless case is represented by exponentially distributed waiting times. Cases of long waiting times with fat-tailed waiting time distributions are considered as well where the SCIRS evolution equations take the form of time-fractional ODEs. We obtain formulae for the endemic equilibrium and a condition of its existence for cases when the waiting time PDFs have existing means. We analyze the stability of healthy and endemic equilibria and derive conditions for which the endemic state becomes oscillatory (Hopf) unstable. In the second part, we implement a simple multiple random walker's approach (microscopic model of Brownian motion of Z independent walkers) with random SCIRS waiting times into computer simulations. Infections occur with a certain probability by collisions of walkers in compartments I and S. We compare the endemic states predicted in the macroscopic model with the numerical results of the simulations and find accordance of high accuracy. We conclude that a simple random walker's approach offers an appropriate microscopic description for the macroscopic model. SCIRS type models open a wide field of applications allowing the identification of pertinent parameters governing the phenomenology of epidemic dynamics such as extinction, convergence to a stable endemic equilibrium, or persistent oscillatory behavior.

Keywords: Epidemic spreading, SCIRS compartment model with memory, ODE's with random delays, waiting time distribution, simple random walks, general fractional calculus

*Corresponding, E-mail: thomas.michelitsch@sorbonne-universite.fr

Contents

1 Introduction **2**

2 Four compartment model **3**
2.1 Basic notions 3
2.2 Memoryless case – exponentially distributed waiting times 5
2.3 Arbitrary waiting time distributions with memory 6
2.4 Long waiting times – the time fractional case 7
2.5 Endemic equilibrium for waiting time PDFs with existing mean 8

3 δ-distributed waiting times **10**
3.1 Stability analysis of endemic and healthy states 11

4 Microscopic model and computer simulations **14**
4.1 Simple random walk model 14
4.2 Validation of the macroscopic SCIRS model and case study 15

5 Conclusions **20**

A General derivatives **21**

B Stability analysis for arbitrary waiting time densities **21**

1 Introduction

The origin of modern epidemic modeling started with the seminal work of Kermack and Mc Kendrick almost a century ago [1]. They introduced the so called 'SIR model' where SIR stands for three compartments characterizing the states of health of an individual, namely S = susceptible, I = infected, R = recovered. The classical SIR model and various generalizations are able to capture some of the features of epidemic spreading of infectious diseases as observed in influenza, measles, mumps, and rubella. In the meantime a huge burst of compartment models and generalizations of the SIR model have been introduced [2, 3].

While the interest in mathematical modeling of epidemic spreading was growing continuously, it is unsurprising that the emergence of the Covid pandemics has launched an enhanced interest and urgent need in advanced epidemic modeling [4]. Many models consider a set of nonlinear ordinary differential equations (ODEs) for the time evolution of the compartment populations where a new direction is about to emerge by combining these models with approaches inspired by network science [6, 7, 5, 8, 9, 10, 11] and fractional dynamics [12, 13, 14, 15, 16].

It has turned out that in many cases epidemics including Covid exhibit quasi-periodic patterns and spontaneous new outbreaks even after longer times of inactivity. Persistent oscillatory characteristics in epidemic dynamics was already pointed out a long time ago in the work of Soper [17]. Indeed, a major drawback of classical SIR type models without memory effects lies in their incapacity to capture (persistent) oscillatory behavior.

The present paper aims to tackle this issue and is a generalization of recent works [10, 11]. In [11] is introduced a SIRS compartment model which takes into account a random duration of immunity R allowing a delayed transition R $\to$ S. What is found that this model is able to capture persistent oscillatory behavior in the number of infected individuals. This feature comes along as oscillatory Hopf instability of the endemic state. In the first part of our paper we extend this model to four compartments as relevant states of health in order to capture a larger variety of epidemics. We consider the four compartments S – susceptible; C – infected but not yet infectious (in the incubation phase); I– infected and infectious (ill); R– recovered and immune. We assume random sojourn times (waiting times) t_C, t_I, t_R an individual once infected spends in each of the compartments C, I, R. The sojourn time t_C in compartment C is

interpreted as incubation time, i.e. the delay between infection and the outbreak of the disease. The sojourn times t_I is the duration of the disease (infected and infectious state) and t_R indicates the immunity period after recovery. It appears natural to assume that these variables are not fixed constants, but individually fluctuating random variables drawn by specific distributions. With these assumptions we derive the SCIRS evolution equations where we focus on several pertinent situations of waiting times with existing and non-existing mean. For waiting time probability density functions (PDFs) with existing mean we derive explicit formulae for the endemic equilibrium and analyze its stability.

In the second part of the paper we combine our SCIRS model with a multiple random walker's approach which is implemented into computer simulations. We present a case study and give numerical evidence that a simple random walk approach ('Brownian motion') offers an appropriate description of the SCIRS dynamics with memory.

2 Four compartment model

2.1 Basic notions

We consider a constant population of $Z = Z_S + Z_C + Z_I + Z_R$ individuals ('random walkers') where $Z_S(t), Z_C(t), Z_I(t), Z_R(t)$ indicate their numbers in the compartments S C I R at time t. We consider here first a continuous time model for $Z \gg 1$ walkers with the compartment population fractions $s(t) = \frac{Z_S(t)}{Z}$, $c(t) = \frac{Z_C(t)}{Z}$, $j(t) = \frac{Z_I(t)}{Z}$, $r(t) = \frac{Z_R(t)}{Z}$. We allow for each walker the following transition pathway:

$$\mathrm{S} \to \mathrm{C} \to \mathrm{I} \to \mathrm{R} \to \mathrm{S}$$

Intuitively we infer that allowing for persistent oscillatory and (quasi-) periodic behavior it is necessary to have a closed (cyclic) pathway S $\to \ldots \to$ S of transitions. We assume that $t_C, t_I, t_R \geq 0$ are mutually *independent* random waiting times an individual spends (after infection) in the compartments C, I, R drawn from specific probability density functions (PDFs) which we prescribe by the kernels $K_C(t), K_I(t), K_R(t)$, respectively. These kernels have to be causal functions[1] with (read $\mathbb{P}$ as 'probability'), for instance

$$\mathbb{P}(t_C \in [\tau, \tau + \mathrm{d}\tau]) = K_C(\tau)\mathrm{d}\tau, \qquad t_C > 0$$

indicates the probability that the incubation time $t_C \in [\tau, \tau + \mathrm{d}\tau]$ which is clearly non-zero only for $\tau \geq 0$ as $t_C \geq 0$. In other words: Given a walker has entered compartment C at $\tau = 0$, then $K_C(\tau)\mathrm{d}\tau$ indicates the probability that this walker leaves compartment C during the infinitesimal interval $[\tau, \tau + \mathrm{d}\tau]$ (by a transition C $\to$ I). We introduce the infection rate $\mathcal{A}(t) = \mathcal{A}(j(t), s(t), t) \geq 0$ (number of infections per walker and unit time or entry rate to the incubated compartment C at time t having of units sec^{-1}). We point out that $\mathcal{A}(t)$ is not a known given function of time t but rather an implicit non-linear function of $s(t), j(t)$, namely

$$\mathcal{A}(t) = \mathcal{A}[s(t), j(t)].$$

This quantity contains macroscopic information on the instantaneous number of collisions of individuals in the 'reactive compartments' S and I and needs to be specified by model assumptions. It is important to point out that $\mathcal{A}(t)$ does not depend on the fractions $c(t), r(t)$ of the 'invisible' compartments C and R.

We assume here the most simple nonlinear form $\mathcal{A}(t) = \beta j(t)s(t)$ where $\beta > 0$ is a constant independent of time where β^{-1} introduces a characteristic time scale. β is also a macroscopic measure for the infection probability in a collision of an S and an I walker. The microscopic picture which we will invoke subsequently and implement into computer simulations indeed

[1] A function $g(t)$ is called 'causal' if $g(t) = 0$ for $t < 0$, i.e. non-zero only for $t \geq 0$.

is that the infection rate is driven by random collisions between infected and susceptible independent random walkers.

With these simple assumptions we can establish model equations governing the time evolution of the fractions $s(t), c(t), j(t), r(t)$. We consider the dynamics starting at time $t = 0$ with an initial condition $s(0) = 1 - j_0$, and $j(0) = j_0$ (many healthy and a few infected walkers) and no incubated or recovered walkers $c(0) = r(0) = 0$. Our (SCIRS)- model evolution equations have the following general structure

$$\begin{aligned}
\frac{d}{dt}s(t) &= -\mathcal{A}(t) + (\mathcal{A} \star K_C \star K_I \star K_R)(t) \\
\frac{d}{dt}c(t) &= \mathcal{A}(t) - (\mathcal{A} \star K_C)(t) \\
\frac{d}{dt}j(t) &= (\mathcal{A} \star K_C)(t) - (\mathcal{A} \star K_C \star K_I)(t) \\
\frac{d}{dt}r(t) &= (\mathcal{A} \star K_C \star K_I)(t) - (\mathcal{A} \star K_C \star K_I \star K_R)(t)
\end{aligned} \tag{1}$$

The sum of these rates is vanishing due to $s(t)+c(t)+j(t)+r(t) = 1$. In order that an epidemics starts, it is necessary that the globally healthy state becomes unstable when the initial state is close to the healthy state with $j_0 \sim \frac{1}{Z} \to 0+$, i.e. where for instance only one infected walker is present at $t = 0$ (among a large population Z). We analyze the stability of the healthy state subsequently in detail. In (1) we have employed the notation

$$(K \star f)(t) = \int_0^t K(t-\tau)f(\tau)\mathrm{d}\tau, \qquad t \geq 0 \tag{2}$$

for convolutions of causal functions $K(t), f(t)$. Be aware that convolutions commute and are associative which can be seen by the representation ($t \geq 0$) of the multiple convolution

$$(K_1 \star K_2 \star \ldots \star K_n)(t) =: \int_{-\infty}^{\infty} \ldots \int_{-\infty}^{\infty} \mathrm{d}\tau_1 \ldots \mathrm{d}\tau_n \delta(t - \tau_1 - \ldots - \tau_n) K_1(\tau_1) \ldots K_n(\tau_n) \tag{3}$$

where $\delta(\ldots)$ indicates the Dirac δ-function and (3) is non-zero only for $t \geq 0$ (causality of the $K_i(\tau)$). Introducing the Laplace transform of our kernels which we define as

$$\hat{K}(\lambda) = \int_0^{\infty} e^{-\lambda t} K(t)\mathrm{d}t$$

where λ indicates the Laplace variable. $\mathcal{K}(\lambda)\Big|_{\lambda=0} = 1$ indicates that the kernels are normalized PDFs. A further observation is worthy of mention. Any (multiple) convolution of PDFs gives again a PDF. This can be easily seen by integrating (3) over time to yield one. Therefore the kernels $K_C(t)$, $(K_C \star K_I)(t)$, $(K_C \star K_I \star K_R)(t)$ which appear in (1) all are (normalized and causal) PDFs representing, respectively the densities of the random variables t_C, $t_C + t_I$, and $t_C + t_I + t_R$. We can see in (1) that for each compartment where an individual remains for a random duration an additional convolution occurs describing the delayed transition out of the compartment. These delayed transitions introduce memory into the rates of individuals leaving the compartments. We will give a careful account for this issue later (subsequent representation (11)).

The interpretation of (1) is as follows. In the first line $\mathcal{A}(t)$ is the rate of infections (transitions S $\to$ C) at time t. The second term $(\mathcal{A} \star K_C \star K_I \star K_R)(t)$ is the rate of individuals losing their immunity (R $\to$ S) having undergone the full pathway of SCIRS transitions. In the second Eq. of (1) $\mathcal{A}(t)$ re-appears as the entry rate to state C. The convolution $(\mathcal{A} \star K_C)(t)$ is the rate of delayed transition C $\to$ I of individuals that fall ill at time t. This rate reappears in the third line of (1) as entry rate into compartment I. Then $(\mathcal{A} \star K_C \star K_I)(t)$ is the rate of recovery I $\to$

R reoccurring in third equation as entry rate into compartment R. Finally $(\mathcal{A} \star K_C \star K_I \star K_R)(t)$ is the rate of individuals losing their immunity (transition I $\to$ S) and re-appears in the first equation as entry rate into S. Let us consider for a moment the second equation in (1) more closely

$$\frac{d}{dt}c(t) = \mathcal{A}(t) - \int_0^t K_C(t-\tau)\mathcal{A}(\tau)\mathrm{d}\tau \tag{4}$$

For our convenience we introduce the 'survival probability' $\Phi_{C,I,R}(t)$ for individuals in compartments C, I, R (also called 'persistence probability' or 'survival function'), e.g. [14] (and many others)

$$\Phi_{C,I,R}(t) = \mathbb{P}(t_{C,I,R} > t) = \int_t^\infty K_{C,I,R}(\tau)\mathrm{d}\tau = 1 - \int_0^t K_{C,I,R}(\tau)\mathrm{d}\tau \tag{5}$$

indicating the probability that an individual which is entering compartment C, I, R, respectively at $t' = 0$ at time $t' = t$ still is ('survives') in this compartment. (5) is capturing all realizations with $t_{C,I,R} > t$ where $\frac{d}{dt}\Phi_{C,I,R}(t) = -K_{C,I,R}(t)$. We observe in this relation the initial condition $\Phi_{C,I,R}(0) = 1$ as a consequence of the normalization of the waiting time PDFs and is telling us that an individual is, with probability one, in a compartment at the instant when entering it. Further we have $\Phi_{C,I,R}(t \to \infty) \to 0+$, i.e. an individual 'survives' only a finite time in compartments C, I, R to enter eventually the susceptible state S. We hence can integrate (4) and rewrite as

$$c(t) = \int_0^t \Phi_C(t-\tau)\mathcal{A}(\tau)\mathrm{d}\tau = (\Phi_C \star \mathcal{A})(t) \tag{6}$$

where initial condition $c(0) = 0$ is assumed. We can also verify this relation by its Laplace transform (subsequent second equation of (9)) and directly by differentiating this expression with respect to t and using the initial condition $\Phi_C(0) = 1$. We interpret (6) as follows: $\mathcal{A}(\tau)\mathrm{d}\tau$ is the fraction of walkers entering C during $[\tau, \tau + \mathrm{d}\tau]$ and $\Phi_C(t-\tau)$ is the (survival-) probability that this fraction still is in C after a delay of $t_C = t - \tau$, i.e. at time instant t where this expression sums up over the complete history of entries into C from 0 to time t. With these considerations we can rewrite our SCIRS Eqs. (1) in the equivalent integral form

$$\begin{aligned} s(t) &= 1 - c(t) - j(t) - r(t) \\ c(t) &= (\Phi_C \star \mathcal{A})(t) \\ j(t) &= j_0 + (\mathcal{A} \star K_C \star \Phi_I)(t) \\ r(t) &= (\mathcal{A} \star K_C \star K_I \star \Phi_R)(t) \end{aligned} \quad , \qquad (t \geq 0) \tag{7}$$

where the initial conditions $s(0) = 1 - j_0$, $c(0) = 0$, $j(0) = j_0$ $r(0) = 0$ are assumed.

2.2 Memoryless case – exponentially distributed waiting times

It is worthy to consider exponential waiting time kernels $K_{C,I,R}(t) = \xi_{C,I,R} e^{-t\xi_{C,I,R}}$ ($\xi_{C,I,R}^{-1} = \langle t_{C,I,R} \rangle$) where the survival functions are also exponentials $\Phi_{C,I,R}(t) = e^{-t\xi_{C,I,R}}$ thus $K_{C,I,R}(t) = \xi_{C,I,R}\Phi_{C,I,R}(t)$. Substituting this into (1) and accounting for (7) takes us to the particular simple form without memory

$$\begin{aligned} \frac{d}{dt}s(t) &= -\mathcal{A}(t) + \xi_R\, r(t) \\ \frac{d}{dt}c(t) &= \mathcal{A}(t) - \xi_C\, c(t) \\ \frac{d}{dt}j(t) &= \xi_C c(t) - \xi_I\,[j(t) - j_0] \\ \frac{d}{dt}r(t) &= \xi_I\,[j(t) - j_0] - \xi_R\, r(t) \end{aligned} \qquad (t \geq 0). \tag{8}$$

Indeed exponential densities stand out by the memoryless feature and the Markov property (see textbooks, e.g. [18] and many others for details), thus the transition rates in (8) depend only on the instantaneous state $s(t), c(t), j(t), r(t)$ but not on the history of the evolution. Setting the transition rates on the left hand side to zero yields straight-forwardly the endemic state which we derive subsequently (Eqs. (21), (22)) for arbitrary waiting time kernels with existing means.

2.3 Arbitrary waiting time distributions with memory

To explore the general cases with memory consider now the equivalent representations (7) and (1) in the Laplace space

$$\begin{aligned}
\hat{s}(\lambda) &= \frac{1-j_0}{\lambda} - \hat{\mathcal{A}}(\lambda)\frac{[1-\hat{K}_C(\lambda)\hat{K}_I(\lambda)\hat{K}_R(\lambda)]}{\lambda} \\
\hat{c}(\lambda) &= \hat{\mathcal{A}}(\lambda)\frac{(1-\hat{K}_C(\lambda)}{\lambda} \\
\hat{j}(\lambda) &= \frac{j_0}{\lambda} + \hat{\mathcal{A}}(\lambda)\hat{K}_C(\lambda)\frac{(1-\hat{K}_I(\lambda)}{\lambda} \\
\hat{r}(\lambda) &= \hat{\mathcal{A}}(\lambda)\hat{K}_C(\lambda)\hat{K}_I(\lambda)\frac{(1-\hat{K}_R(\lambda)}{\lambda}
\end{aligned} \tag{9}$$

where all Laplace transforms (LTs) depend on $\hat{\mathcal{A}}(\lambda)$ of the (unknown) infection rate and $\hat{\Phi}_{C,I,R}(\lambda) = \frac{(1-\hat{K}_{C,I,R}(\lambda)}{\lambda}$ are the LTs of the survival probabilities. We further have that

$$\hat{s}(\lambda) + \hat{c}(\lambda) + \hat{j}(\lambda) + \hat{r}(\lambda) = \frac{1}{\lambda} = \int_0^\infty e^{-\lambda t}\mathrm{d}t$$

as we deal with a constant population. We observe that in the first Eq. of (9) the term $\frac{[1-\hat{K}_C(\lambda)\hat{K}_I(\lambda)\hat{K}_R(\lambda)]}{\lambda}$ is the LT of the survival probability $\mathbb{P}[t_C + t_R + t_I > t]$ (due to the PDF $(K_c \star K_I \star k_R)(t)$ of the random variable $t_C + t_I + t_R$), corresponding to individuals 'surviving' in one of the compartments C, I, R at time t. To shed more light on how the memory comes into play we introduce a 'memory operator' (For our convenience we employ here a slightly modified definition as in [14, 26].)[2]

$$\hat{\mathcal{M}}(\lambda) = \frac{\hat{K}(\lambda)}{\hat{\Phi}(\lambda)} = \lambda\frac{\hat{K}(\lambda)}{1-\hat{K}(\lambda)} = \lambda\hat{\mathcal{L}}(\lambda). \tag{10}$$

Then reading $\hat{K}(\lambda) = \mathcal{M}(\lambda)\hat{\Phi}(\lambda)$ as convolutions in the time domain we can rewrite our SCIRS Eqs. (1) (in the Caputo sense) of general (fractional) derivatives (see [29, 15, 16] and Appendix) as

$$\begin{aligned}
\frac{d}{dt}s(t) &= -\mathcal{A}(t) + \int_0^t \mathcal{L}_R(t-\tau)\frac{d}{d\tau}r(\tau)\mathrm{d}\tau \\
\frac{d}{dt}c(t) &= \mathcal{A}(t) - \int_0^t \mathcal{L}_C(t-\tau)\frac{d}{d\tau}c(\tau)\mathrm{d}\tau \\
\frac{d}{dt}j(t) &= \int_0^t \mathcal{L}_C(t-\tau)\frac{d}{d\tau}c(\tau)\mathrm{d}\tau - \int_0^t \mathcal{L}_I(t-\tau)\frac{d}{d\tau}j(\tau)\mathrm{d}\tau \\
\frac{d}{dt}r(t) &= \int_0^t \mathcal{L}_I(t-\tau)\frac{d}{d\tau}j(\tau)\mathrm{d}\tau - \int_0^t \mathcal{L}_R(t-\tau)\frac{d}{d\tau}r(\tau)\mathrm{d}\tau.
\end{aligned} \tag{11}$$

These equations show that the transition rates at time t have a complete memory of their previous values. Alternatively we can write (11) in the Riemann-Liouville manner of general

[2] We suppress here subscripts C, I, R.

fractional derivatives (see Appendix). For exponential waiting time PDFs $K_{exp}(t) = \xi e^{-\xi t}$ we have $\hat{\mathcal{M}}_{exp}(\lambda) = \xi$ thus $\mathcal{M}_{exp}(t) = \xi\delta(t)$ (i.e. is null for $t > 0$ indicating lack of memory) and we easily recover above memoryless SCIRS Eqs. (8).

2.4 Long waiting times – the time fractional case

Representation (11) is especially useful when we deal with fat-tailed waiting time PDFs without existing means such as the Mittag-Leffler waiting-time PDF (ML-PDF) which (see [28] and references therein for explicit formulas). The ML-PDF is a fractional generalization of the exponential PDF and has the LT [14, 26] (and many others)

$$\tilde{K}_\beta(\lambda) = \frac{\xi}{\xi + \lambda^\beta}, \qquad \beta \in (0,1), \quad \xi > 0 \tag{12}$$

where due to the fat tail the mean waiting time $-\frac{d}{d\lambda}\tilde{K}_\beta(\lambda)\Big|_{\lambda=0} \to \infty$ does not exist as $\beta \in (0,1)$ (occurrence of extremely long waiting times). For $\beta = 1$ (12) retrieves the LT of the exponential density. Expanding the LT for λ small $\tilde{K}_\beta(\lambda) \sim 1 - \frac{\lambda^\beta}{\xi}$, Laplace inversion shows that ML-PDF has a fat power law tail $K_\beta(t) \sim \frac{\beta}{\Gamma(1-\beta)}\frac{t^{-\beta-1}}{\xi}$ $(t \to \infty)$ corresponding to a long memory. For the ML-case we have for (10)

$$\hat{\mathcal{L}}_\beta(\lambda) = \xi\lambda^{-\beta} \tag{13}$$

where $\lambda^{-\beta}$ corresponds to the Riemann-Liouville fractional integral of degree β and $\hat{\mathcal{M}}_\beta(\lambda) = \xi\lambda^{1-\beta}$ the Riemann -Liouville (R-L) fractional derivative of order $1-\beta$. Denoting D_t^ν the R-L fractional derivative where it is sufficient here to consider the range $\mu \in (0,1)$ defined by [28]

$$D_t^\mu \cdot f(t) = \frac{d}{dt}\int_0^t \frac{(t-\tau)^{-\mu}}{\Gamma(1-\mu)} f(\tau)\mathrm{d}\tau, \qquad \mu \in (0,1) \tag{14}$$

having LT $\lambda^\mu \hat{f}(\lambda)$ and with the definition of the Caputo fractional derivative

$$\frac{d^\mu}{dt^\mu} f(t) = \int_0^t \frac{(t-\tau)^{-\mu}}{\Gamma(1-\mu)}\frac{d}{d\tau} f(\tau)\mathrm{d}\tau = D_t^\mu \cdot f(t) - f(0)\frac{t^{-\mu}}{\Gamma(1-\mu)}, \qquad \mu \in (0,1) \tag{15}$$

with LT $\lambda^\mu \hat{f}(\lambda) - f(0)\lambda^{\mu-1}$. Consult the Appendix and [29] for the connections with general (fractional) derivatives. In the limit $\mu \to 1-$ both Caputo and RL-fractional derivatives converge to the first order standard derivative where $\frac{t^{-\mu}}{\Gamma(1-\mu)} \to \delta(t)$. Using the feature

$$\frac{d^\mu}{dt^\mu}[f(t) - f(0)] = \frac{d^\mu}{dt^\mu} f(t) = D_t^\mu \cdot [f(t) - f(0)] \tag{16}$$

we can then write (11) when all waiting times $t_{C,I,R}$ are drawn from ML PDFs in terms of Caputo fractional derivatives as

$$\begin{aligned}
\frac{d}{dt}s(t) &= -\mathcal{A}(t) + \xi_R \frac{d^{1-\beta}}{dt^{1-\beta}} r(t) \\
\frac{d}{dt}c(t) &= \mathcal{A}(t) - \xi_C \frac{d^{1-\beta}}{dt^{1-\beta}} c(t) \\
\frac{d}{dt}j(t) &= \xi_C \frac{d^{1-\beta}}{dt^{1-\beta}} c(t) - \xi_I \frac{d^{1-\beta}}{dt^{1-\beta}} j(t) \\
\frac{d}{dt}r(t) &= \xi_I \frac{d^{1-\beta}}{dt^{1-\beta}} j(t) - \xi_R \frac{d^{1-\beta}}{dt^{1-\beta}} r(t)
\end{aligned} \tag{17}$$

retrieving for $\beta = 1$ the Eqs. (8) of exponential waiting time PDFs (see (15), (16)). Indeed the time-fractional case with fat-tailed waiting time distributions is of utmost importance deserving further thorough investigation, see Appendix B for a brief account.

2.5 Endemic equilibrium for waiting time PDFs with existing mean

Here we confine ourselves to waiting time PDFs with existing means. The endemic state is defined as the long-time limit of the evolution. That is we seek a stationary (constant solution) $[s(t), c(t), j(t), r(t)] \to [S_e, C_e, J_e, R_e]$ and $\mathcal{A}(t) \to A_e = \beta J_e S_e$ which also is the asymptotic solution for $t \to \infty$ if the endemic state is stable. This solution can be obtained from Eqs. (9) in the limit of small λ, where these equations then take (with $\hat{s}(\lambda) \to S_e/\lambda$,..) the form

$$\begin{aligned} S_e &= 1 - j_0 - \lim_{\lambda\to 0} \hat{\mathcal{A}}(\lambda)[1 - K_C(\lambda)K_I(\lambda)\hat{K}_R(\lambda)] \\ C_e &= \lim_{\lambda\to 0} \hat{\mathcal{A}}(\lambda)[1 - \hat{K}_C(\lambda)] \\ J_e &= j_0 + \lim_{\lambda\to 0} \hat{\mathcal{A}}(\lambda)\hat{K}_C(\lambda)[1 - \hat{K}_I(\lambda)] \\ R_e &= \lim_{\lambda\to 0} \hat{\mathcal{A}}(\lambda)\hat{K}_C(\lambda)\hat{K}_I(\lambda)[1 - \hat{K}_R(\lambda)] \end{aligned} \tag{18}$$

with

$$\hat{\mathcal{A}}(\lambda) \approx \frac{A_e}{\lambda} + A_0 + A_1\lambda + \dots$$

which has to be considered for $\lambda \to 0$ where the lowest order in λ determines the endemic equilibrium. Now with

$$\hat{K}(\lambda) = \int_0^\infty e^{-\lambda\tau} K(\tau)\mathrm{d}\tau \approx \int_0^\infty [1 - \lambda\tau]K(\tau)\mathrm{d}\tau + o(\lambda) = 1 - \lambda\langle\tau\rangle + o(\lambda) \tag{19}$$

where with $\langle..\rangle$ we denote mean values and $o(\lambda)$ stands for the Landau symbol. Thus we have

$$\hat{K}_{C,I,R}(\lambda) = 1 - \lambda\langle t_{C,I,R}\rangle + o(\lambda) \tag{20}$$

and $\hat{K}_C(\lambda)\hat{K}_I(\lambda)\hat{K}_R(\lambda) = 1 - \lambda\langle t_C + t_I + t_R\rangle + o(\lambda) = 1 - \lambda\langle T\rangle + o(\lambda)$ and as said we assume that the means exist. Therefore,

$$\lim_{\lambda\to 0} \hat{\Phi}_{C,I,R}(\lambda) = \lim_{\lambda\to 0} \frac{(1 - \hat{K}_{C,I,R}(\lambda)}{\lambda} = -\frac{d}{d\lambda}\hat{K}_{C,I,R}(\lambda)\Big|_{\lambda=0} = \langle t_{C,I,R}\rangle$$

Then we get straight-forwardly for the lowest orders in λ the endemic equilibrium as follows

$$\begin{aligned} S_e &= 1 - j_0 - A_e\,\langle T\rangle \\ C_e &= A_e\,\langle t_C\rangle \\ J_e &= j_0 + A_e\langle t_I\rangle \\ R_e &= A_e\,\langle t_R\rangle \end{aligned} \tag{21}$$

and with our assumption $A_e = \beta J_e S_e$ we arrive at

$$\begin{aligned} S_e(J_e) &= \frac{1 - j_0}{1 + \beta\langle\, T\,\rangle J_e} \\ C_e(J_e) &= \frac{(1 - j_0)\beta\langle t_C\rangle J_e}{1 + \beta\langle\, T\,\rangle J_e} \\ J_e &= j_0 + \beta\langle t_I\rangle J_e \frac{1 - j_0}{1 + \beta\langle T\rangle J_e} \\ R_e(J_e) &= \frac{(1 - j_0)\beta\langle t_R\rangle J_e}{1 + \beta\langle\, T\,\rangle J_e}. \end{aligned} \tag{22}$$

Consider now the third relation in (22) which is an implicit equation for J_e leading to

$$J_e^2 - 2aJ_e - b = 0 \tag{23}$$

where we have introduced

$$\begin{aligned} a &= \frac{j_0}{2} + \frac{\beta\langle t_I\rangle(1-j_0)-1}{2\beta\langle T\rangle} = \frac{\langle t_R + t_C\rangle)j_0}{2\langle T\rangle} + \frac{R_0-1}{2\beta\langle T\rangle}, \qquad R_0 = \beta\langle t_I\rangle \\ b &= \frac{j_0}{\beta\langle T\rangle}. \end{aligned} \tag{24}$$

The quantity $R_0 = \beta\langle t_I\rangle$ can be interpreted as the 'basic reproduction number' and is a crucial (control-) parameter. (23) has the roots

$$(J_e)_{1,2} = a \pm \sqrt{a^2+b}. \tag{25}$$

Clearly the endemic equilibrium exists only for those roots with $J_e \in [0,1]$ where the full endemic state then is determined by (22). For $b = 0$ ($j_0 = 0$) one root is zero corresponding to the healthy state $S_e = 1$. The second root is $J_e(j_0 = 0) = 2a = \frac{R_0-1}{\beta\langle T\rangle} \in [0,1)$ for $R_0 = \beta\langle t_I\rangle > 1$ which therefore is the condition of the existence of an endemic state for $j_0 = 0$. In Appendix B we show for waiting time PDFs with existing means that $R_0 > 1$ also is the condition that the healthy state is unstable thus an epidemic can start to spread. We also show there that the healthy state is always unstable if $K_I(t)$ has a fat tail (i.e. infinite mean). Indeed for $\langle t_I\rangle \to \infty$ (β, t_C, t_R kept finite) we have $R_0 \to \infty$ thus $J_e(j_0 = 0) \sim \langle t_I\rangle/\langle T\rangle \to 1$ and for $\beta \to \infty$ ($\langle t_I\rangle, \langle t_C\rangle, \langle t_R\rangle$ finite) we get $J_e(j_0 = 0) \to \langle t_I\rangle/\langle T\rangle$.

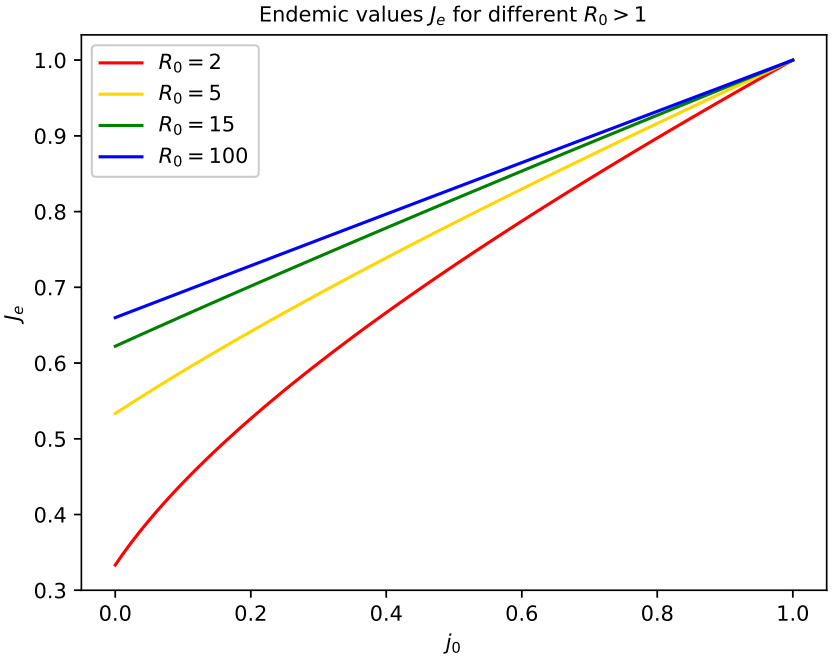

Figure 1: Endemic value $J_e(j_0, R_0)$ vs j_0 from Eq. (26) with (24) for different values of $R_0 > 1$ where in all curves we have put $\langle t_C\rangle = \langle t_R\rangle = 5$, $\langle t_I\rangle = 20$.

Consider now $j_0 > 0$ and $R_0 > 1$. Then we have $a < 1$ as $\frac{\langle t_R+t_C\rangle j_0}{2T} < \frac{1}{2}$ and $\frac{R_0-1}{2\beta\langle T\rangle} < \frac{1}{2}$ and $b < 1$ thus only the positive root is

$$(J_e)_1 = a + \sqrt{a^2+b} \tag{26}$$

whereas the other $(J_e)_2 = a - \sqrt{a^2+b} < 0$. The endemic state exists if $(J_e)_1 \leq 1$. As a, b are monotonously increasing functions of j_0 let us check the root for the maximum value $j_0 = 1$ where $a(j_0 = 1) = \frac{1}{2} - \frac{1}{2\beta T} = \frac{1}{2}(1-\epsilon)$ and $b(j_0 = 1) = \frac{1}{\beta\langle T\rangle} = \epsilon$. Then we get

$$J_e(j_0)\Big|_{j_0=1} = \frac{1}{2}(1-\epsilon+\sqrt{(1-\epsilon)^2+4\epsilon} = \frac{1-\epsilon+\sqrt{(1+\epsilon)^2}}{2} = 1 \tag{27}$$

i.e. the initial and endemic state coincide $j_0 = J_e(1) = 1$ where we infer that $j = 1$ (for $R_0 > 1$) should be a stable endemic state. From the monotony of $J_e(j_0)$ (see (24)) we can see that

$$\frac{R_0 - 1}{\beta\langle T\rangle} \leq J_e(j_0) \leq J_e(j_0)\Big|_{j_0=1} = 1$$

i.e. in the entire range $j_0 \in [0, 1]$ the endemic value is given by the positive root (26) together with (24). This behavior is shown in the plot of Figure 1 where we draw J_e versus j_0 for different values of $R_0 > 1$. One can see that J_e is monotonously increasing with R_0 when $\langle t_R\rangle, \langle t_C\rangle, j_0$ are kept constant.

We focus now on initial conditions $s_0 = 1-$ and $j_0 = 0+$ (healthy state). The endemic equilibrium (22) then writes

$$\begin{aligned} S_e &= \frac{1}{R_0} \\ C_e &= \frac{R_0-1}{R_0}\frac{\langle t_C\rangle}{\langle T\rangle} \\ J_e &= \frac{R_0-1}{R_0}\frac{\langle t_I\rangle}{\langle T\rangle} \\ R_e &= \frac{R_0-1}{R_0}\frac{\langle t_R\rangle}{\langle T\rangle} \end{aligned} \qquad (\langle T\rangle = \langle t_C + t_I + t_R\rangle, \qquad R_0 = \beta\langle t_I\rangle) \tag{28}$$

and exists solely for $R_0 > 1$ depending only from R_0 and the mean waiting times $\langle t_{C,I,R}\rangle$. We may consider the following limiting cases.
1) $\langle t_R\rangle \to \infty$ (infinitely long immunity), $\langle t_C\rangle, \langle t_I\rangle, \beta$ are kept constant:
Then we have $\frac{\langle t_R\rangle}{\langle T\rangle} \to 1$ and $\frac{\langle t_C\rangle}{\langle T\rangle}, \frac{\langle t_I\rangle}{\langle T\rangle} \to 0$ and hence $S_e = \frac{1}{R_0}$ remains unchanged thus $C_e, J_e \to 0$ and $R_e \to \frac{R_0-1}{R_0}$ with $S_e + R_e = 1$ which corresponds to a fully healthy population (susceptible or immune) with $C_e + J_e \to 0$, i.e. the disease in the long time limit dies out.
2) In the same way the limits $\langle t_I\rangle \to \infty$ (long illness time) and and long incubation time $\langle t_C\rangle \to \infty$, respectively, are straightforward, where the endemic values of respective compartments with infinite waiting times tend to $\frac{R_0-1}{R_0}$ with unchanged $S_e = \frac{1}{R_0}$. This corresponds to the fact that the individuals remain eventually trapped in the respective compartments (C or I) with infinite waiting times thus the cyclic transition pathway $S \to \ldots \to S$ is suppressed. We infer that in the limiting cases 1), 2) the endemic states are stable similar to the class of classical SIR models and do not exhibit oscillatory instabilities.

3 δ-distributed waiting times

An instructive case consists in the deterministic limit when the sojourn times in the compartments for all walkers are constant. Then the waiting time PDFs are Dirac δ-functions

$$K_{C,I,R}(t) = \delta(t - t_{C,I,R}) \tag{29}$$

with LTs $\hat{K}_{C,I,R}(\lambda) = e^{-\lambda t_{C,I,R}}$. Recall now the convolution of two δ-kernels

$$\delta(t-t_1) \star \delta(t-t_1) = \delta(t-t_1-t_2)$$

which yields a new δ-kernel with a shifted peak at $t_1 + t_2$. With this observation we have $(K_C \star K_I)(t) = \delta(t - t_C - t_I)$ and $(K_C \star K_I \star K_R)(t) = \delta(t - t_C - t_I - t_R)$. Then the SCIRS equations (1) read

$$\begin{aligned} \tfrac{d}{dt}s(t) &= -\mathcal{A}(t) + \mathcal{A}(t - t_C - t_I - t_R) \\ \tfrac{d}{dt}c(t) &= \mathcal{A}(t) - \mathcal{A}(t - t_C) \\ \tfrac{d}{dt}j(t) &= \mathcal{A}(t - t_C) - \mathcal{A}(t - t_C - t_I) \\ \tfrac{d}{dt}r(t) &= \mathcal{A}(t - t_C - t_I) - \mathcal{A}(t - t_C - t_I - t_R). \end{aligned} \tag{30}$$

Note that $\mathcal{A}(t) = \mathcal{A}[j(t), s(t)]$ is causal, i.e. all functions with negative time arguments are vanishing. For $t < t_C$ the infected individuals accumulate in the compartment C and for $t \geq t_C$ some start to leave compartment C to enter I with the delayed rate $A(t - t_C)$. Then for $t \geq t_C + t_I$ the first individuals are healed starting transitions I $\to$ R with rate $A(t - t_C - t_I)$. Finally for $t \geq t_C - t_I - t_R$ the transitions R $\to$ S due to individuals losing their immunity occur. From these observations we can infer that

$$\begin{aligned} c(t) = &\int_0^t \mathcal{A}(\tau)\,\mathrm{d}\tau - \Theta(t - t_C)\int_0^{t-t_C} \mathcal{A}(\tau)\,\mathrm{d}\tau \\ j(t) = &\, j_0 + \Theta(t - t_C)\int_0^{t-t_C} \mathcal{A}(\tau)\,\mathrm{d}\tau - \Theta(t - t_C - t_I)\int_0^{t-t_C-t_I} \mathcal{A}(\tau)\,\mathrm{d}\tau \\ r(t) = &\, \Theta(t - t_C - t_I)\int_0^{t-t_C-t_I} \mathcal{A}(\tau)\,\mathrm{d}\tau - \Theta(t - t_C - t_I - t_R)\int_0^{t-t_C-t_I-t_R} \mathcal{A}(\tau)\,\mathrm{d}\tau \end{aligned} \tag{31}$$

where $\Theta(\tau)$ denotes the Heaviside unit step function defined as $\Theta(\tau) = 1$ for $\tau \geq 0$ and $\Theta(\tau) = 0$ for $\tau < 0$. We can see for sharp waiting times the Heaviside functions 'switch on and off' the respective transitions between compartments. It is worthy of mention that (31) is consistent with (7) when we take into account the survival probabilities

$$\Phi_{C,I,R}(t) = \int_t^\infty \delta(\tau - t_{C,I,R})\mathrm{d}\tau = \Theta(t_{C,I,R} - t) = 1 - \Theta(t - t_{C,I,R}) \tag{32}$$

i.e. $\Phi_{C,I,R}(t) = 1$ for $t < t_{C,I,R}$ ('survival' in C, I, R, respectively) and $\Phi_{C,I,R}(t) = 0$ for $t > t_{C,I,R}$ ('death', having left C, I, R, respectively). From Eqs. (31) we find the endemic equilibrium S_e, C_e, J_e, R_e representing a stationary solution of (30). Plugging the stationary value $\mathcal{A}_e = \beta J_e S_e$ into (31) we re-arrive at Eqs. (22) with $t_{C,I,R} = \langle t_{C,I,R} \rangle$ for Dirac δ-distributions.

3.1 Stability analysis of endemic and healthy states

Here we investigate the stability of the endemic equilibrium for healthy initial conditions $s_0 = 1$ ($j_0 = 0$) for δ-distributed waiting times. To this end we set

$$\begin{aligned} s(t) &= S_e + ue^{\mu t} \\ c(t) &= C_e + ve^{\mu t} \\ j(t) &= J_e + we^{\mu t} \\ r(t) &= R_e + xe^{\mu t} \end{aligned} \tag{33}$$

where u, v, w, x are 'small' time independent constants. Clearly at least one of these equations is redundant as $s + c + j + r = 1$. Then it follows that $\mathcal{A}(t) \approx A_e + A_0(u, w)e^{\mu t}$ where we take into

account only the linear orders in u, v, w, x. Therefore, $A_e = \beta J_e S_e$ and $A_0(u, w) = \beta(uJ_e + wS_e)$. Plugging this into (30) leads to the following system of equations

$$\begin{aligned} A_0(u,w)(1-e^{-\mu T}) + \mu u &= 0 \\ A_0(u,w)(1-e^{-\mu t_C}) - \mu v &= 0 \\ A_0(u,w)e^{-\mu t_C}(1-e^{-\mu t_I}) - \mu w &= 0 \\ A_0(u,w)e^{-\mu(t_C+t_I)}(1-e^{-\mu t_R}) - x\mu &= 0. \end{aligned} \tag{34}$$

We can eliminate $v = A_0(u, w)\frac{1-e^{-\mu t_C}}{\mu}$ and $x = A_0(u, w)e^{-\mu(t_C+t_I)}\frac{1-e^{-\mu t_R}}{\mu}$ which are uniquely determined by u and w. Therefore the solvability condition is determined uniquely by the first and third equation for s and j containing only the coefficients u and w. The complete determinant of the system (34) leads to

$$\left\| \begin{array}{ll} \beta J_e(1-e^{-\mu T}) + \mu; & \beta S_e(1-e^{-\mu T}) \\ \beta J_e e^{-\mu t_C}(1-e^{-\mu t_I}); & \beta S_e e^{-\mu t_C}(1-e^{-\mu t_I}) - \mu \end{array} \right\| \mu^2 = 0. \tag{35}$$

We have $\mu = 0$ as a threefold eigenvalue and with one non-zero eigenvalue μ_1 determined by

$$\mu = \beta S_e e^{-\mu t_C}(1-e^{-\mu t_I}) - \beta J_e(1-e^{-\mu T}) \tag{36}$$

and hence $\mu_1 = \mu_1(\beta, j_0, t_C, t_I, t_R)$. However, we will see that we can reduce the set of pertinent parameters. For the outbreak of an epidemic, it is necessary that the healthy (initial) state $s_0 = 1$ becomes unstable. To explore this issue we consider $s(t) = s_0 + ue^{\mu t}$ and $j(t) = j_0 + we^{\mu t}$ with $s_0 = 1$, $j_0 = 0$. Then we get the solvability condition by replacing in (35) $J_e \to j_0 = 0$ and $S_e \to s_0 = 1$ in the form

$$\tilde{\mu} = R_0 e^{-\tilde{\mu} t_1}[1-e^{-\tilde{\mu}}) = g(\tilde{\mu}, R_0) \tag{37}$$

where we introduce

$$\tilde{\mu} = t_I \mu, \quad t_1 = \frac{t_C}{t_I}, \quad t_2 = \frac{T}{t_I} = 1 + t_1 + \frac{t_R}{t_I}. \tag{38}$$

The healthy state becomes unstable if there is a positive solution $\tilde{\mu}_0 > 0$ of this equation. Clearly there is a positive root only if $\frac{d}{d\tilde{\mu}} g(\tilde{\mu}, R_0)|_{\tilde{\mu}=0} = R_0 > 1$, otherwise the healthy state is stable. This justifies our interpretation of R_0 as the basic reproduction number where the healthy state is unstable for $R_0 > 1$ thus the epidemic starts to spread. In Appendix B we show that the condition for an outbreak $R_0 = \beta\langle t_I\rangle > 1$ holds true for waiting time PDFs with existing means. This can be seen more closely as the right-hand side $g(\tilde{\mu}, R_0)$ of (37) is a concave function of $\tilde{\mu}$ (see Figure 2). We have for $\tilde{\mu}$ small the expansion $g(\tilde{\mu}, R_0) = R_0\tilde{\mu} + O(\tilde{\mu}^2) > \tilde{\mu}$ only if $R_0 > 1$ and always $g(\tilde{\mu}, R_0) \to 0 < \tilde{\mu}$ as $\mu \to \infty$. Therefore exists a positive root $\mu_0(R_0) > 0$ only for $R_0 > 1$. This behavior is sown in Figure 2 where $\mu_0(R_0)$ increases monotonically with R_0 enhancing the (non-persistent) exponential growth of $j(t)$ at the outbreak of the epidemic.

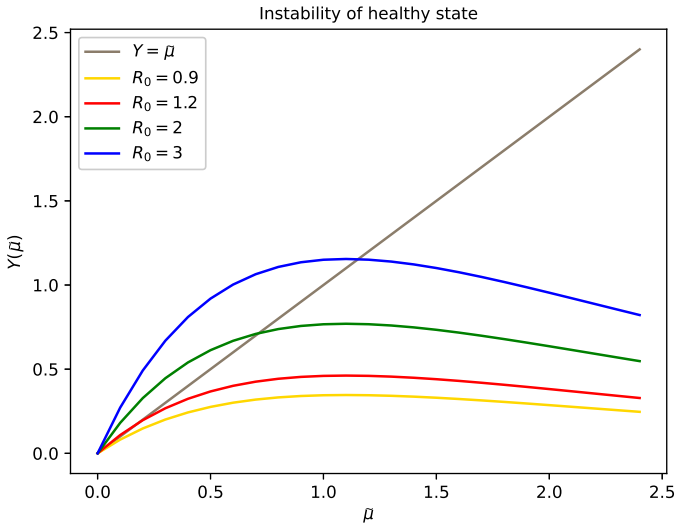

Figure 2: We depict $g(\tilde{\mu}, R_0) = R_0 e^{-\tilde{\mu}t_1}(1 - e^{-\tilde{\mu}})$ for different values of R_0. For $R_0 = 0.9$ (lower curve) the healthy state is stable. In the other curves $R_0 > 1$ the healthy state is unstable. In all plots we chose $t_1 = t_C/t_I = 0.5$.

Returning to the stability analysis of the endemic state we re-scale (36) with (38) as

$$\tilde{\mu} = R_0 S_e e^{-\tilde{\mu}t_1}(1 - e^{-\tilde{\mu}}) - R_0 J_e(1 - e^{-\tilde{\mu}t_2}). \tag{39}$$

At threshold of an oscillatory instability, the eigenvalue is purely imaginary. Plugging $\tilde{\mu} = i\omega$ into (39) and separating real and imaginary parts yields the two conditions

$$\begin{aligned} f_1(r_0, \omega) &= \cos\omega t_1 - \cos\omega(t_1 + 1) - r_0(1 - \cos\omega t_2) &= 0 \\ f_2(r_0, \omega) &= \omega + \sin\omega t_1 - \sin\omega(t_1 + 1) + r_0 \sin\omega t_2 &= 0 \end{aligned} \tag{40}$$

which need to be both simultaneously fulfilled for an oscillatory (Hopf) instability where we introduced the reduced control parameter $r_0 = J_e R_0 = (R_0 - 1)/t_2$.

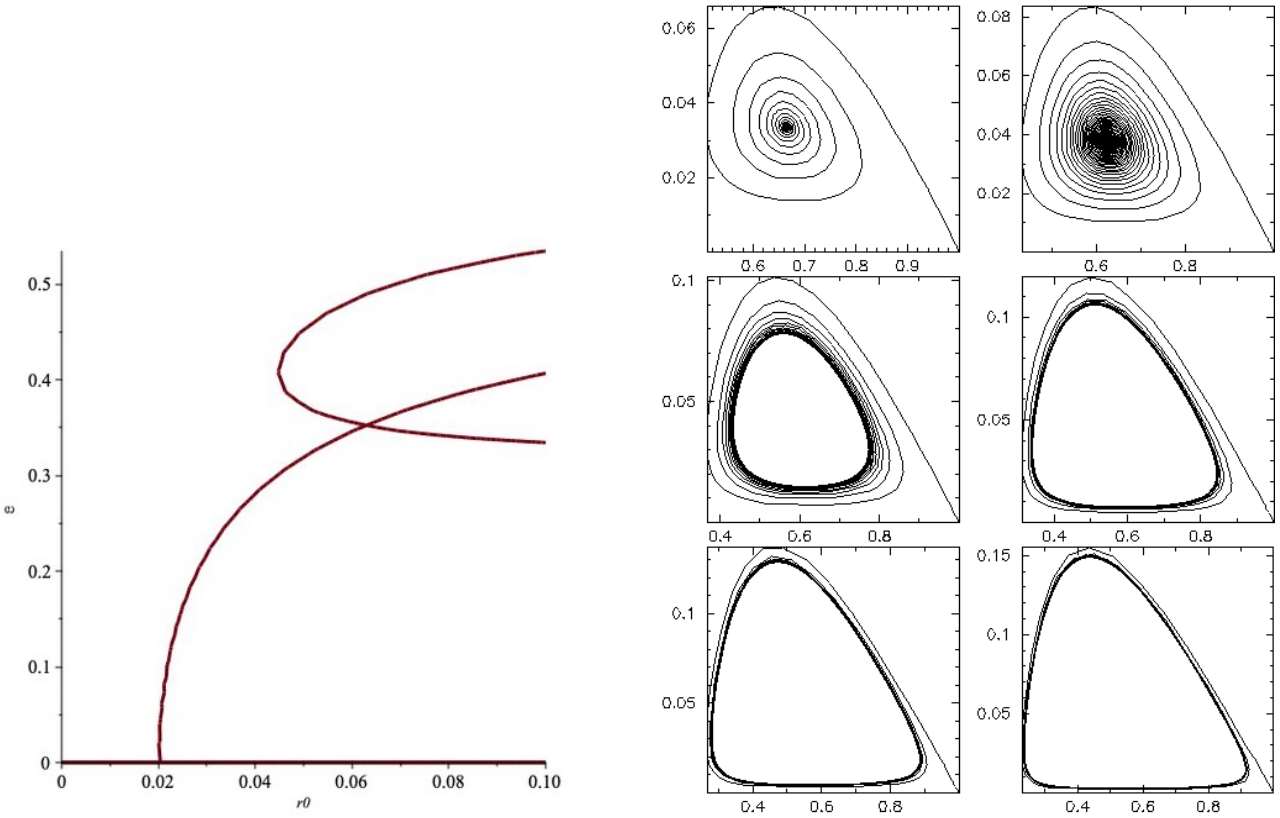

Figure 3: Left: the intersection of the contour lines of $f_1, f_2 = 0$ of (40) yield $(\omega, r_0) \approx (0.5, 0.063)$. Right: numerical solutions of the fully nonlinear delay system (30) for $R_0 = 1.5$ (top left) to $R_0 = 2.0$ in the (j, s)-plane. A limit cycle is born at $R_0 \approx 1.63$.

In Figure 3 (left frame) we plot the zero lines of f_i in the r_0, ω plane for $t_1 = 1/2,\ t_2 = 10$. They intersect at $r_0 \approx 0.063,\ \omega = 0.35$, corresponding to a critical $R_0 \approx 1.63$. The right frame of Figure 3 shows numerical solutions of the full delay system (30) with the same parameters $t_1,\ t_2$. The system is solved using an Euler forward scheme with fixed time step $\delta t = 10^{-4}$. The initial conditions are $j_0 = 10^{-4},\ s_0 = 1 - j_0,\ r_0 = c_0 = 0$ close to the healthy state. We varied R_0 from 1.5 (subcritical, upper left) to 2.0 (lower right frame). Clearly for $R_0 = 1.7$ the stable focus turns into a limit cycle that becomes wider with increasing R_0.

4 Microscopic model and computer simulations

4.1 Simple random walk model

To explore the SCIRS phenomenology we combine this model with a multiple random walker's approach which we implemented into a Python code [30]. In this random walk Z walkers navigate independently on a periodic two dimensional lattice. Each walker performs at integer times $t = 0, 1, 2, \ldots$ instantaneous independent random steps to a closest neighbour lattice point (simple walk). The position of walker j $(j = 1, \ldots Z)$ can be described by the random variables

$$\begin{aligned} x_j(t) &= x_j(t-1) + \eta_x^{(j)}(t) \\ y_j(t) &= y_j(t-1) + \eta_y^{(j)}(t) \end{aligned} \quad , \qquad t = 1, 2, \ldots \tag{41}$$

with the random steps

$$\left(\eta_x^{(j)}(t), \eta_y^{(j)}(t)\right) = (1,0);\ (-1,0);\ (0,1);\ (0,-1) \ \text{ occurring with probability } \frac{1}{4}.$$

This simple multi-walkers motion is a microscopic model with scaling limits to (standard) Brownian motion [27]. We assume a $N_x = N_y = N$-periodic lattice with $x^{(j)}(t) = x^{(j)}(t) \bmod N$,

$y^{(j)}(t) = y^{(j)}(t) \bmod N$ for the position of each walker j. In order to connect the random walk with the epidemic dynamics we apply the following infection rule [11]: If a walker $j \in$ I meets a walker $k \in$ S on the same lattice point ('collision' of an infected–infectious and a susceptible walker), i.e.

$$\begin{aligned} & j \in I \quad \wedge \; k \in S \\ \wedge \quad & x_j(t) = x_k(t) \\ \wedge \quad & y_j(t) = y_k(t) \end{aligned} \tag{42}$$

then the susceptible walker k gets infected with probability P_{inf} and undergoes an instantaneous transition S $\to$ C followed by the transition pathway as described previously. The infection probability P_{inf} is constant for all walkers and time independent. The random paths of the walkers are not affected by transitions between the compartments or 'collisions' of walkers. In the simulations at each integer time instant t we count the populations $Z_{S,C,I,R}(t)$ in the compartments where the total population $Z = Z_S(t) + Z_C(t) + Z_I(t) + Z_R(t)$ remains constant over time. As in the macroscopic model we focus on the fractions $s(t) = Z_S(t)/Z$, $c(t) = Z_C(t)/Z$, $j(t) = Z_I(t)/Z$, $r(t) = Z_R(t)/Z$.

We implement the mutually independent waiting times $t_{C,I,R}$ as random numbers drawn from specific Gamma PDFs $K_{C,I,R}(t)$. The Gamma-distribution provides sufficient flexibility to generate a wide range of possible behaviors such as sharp δ-peaks, broadly scattered waiting times with a maximum or a monotonically decreasing PDF. The Gamma (also called Erlang-) PDF writes

$$K_{\xi,\alpha}(\tau) = \frac{\xi^\alpha \tau^{\alpha-1}}{\Gamma(\alpha)} e^{-\xi\tau}, \qquad \alpha, \xi > 0 \tag{43}$$

where α is the so-called shape parameter and $1/\xi$ the time scale parameter. The Gamma PDF has a maximum for $\alpha > 1$ at $t_m = \frac{\alpha-1}{\xi}$ and is monotonically decreasing for $\alpha \leq 1$ and weakly singular at $t = 0$ for $\alpha < 1$. For $\alpha = 1$ we get the exponential PDF $K_{\xi,1}(\tau) = \xi e^{-\xi\tau}$. Some cases of Gamma PDFs are drawn in histograms of Figure 4. Useful is its Laplace transform

$$\hat{K}_{\xi,\alpha}(\lambda) = \int_0^\infty e^{-\lambda\tau} K_{\xi,\alpha}(\tau) \mathrm{d}\tau = \frac{\xi^\alpha}{(\lambda+\xi)^\alpha} \tag{44}$$

from which we can easily retrieve
$\hat{K}_{\xi,\alpha}(\lambda)\big|_{\lambda=0} = 1$ (normalization), $\langle t \rangle = -\frac{d}{d\lambda}\hat{K}_{\xi,\alpha}(\lambda)\big|_{\lambda=0} = \frac{\alpha}{\xi}$ (mean waiting time), and
$\mathcal{V} = \langle t^2 \rangle - \langle t \rangle^2 = \frac{\alpha}{\xi^2}$ (variance). We use in the simulations to generate constant (sharp) waiting times the feature, e.g. [11]

$$\lim_{\xi\to\infty} K_{\xi,\alpha=\xi\tau_0}(\tau) = \delta(t - \tau_0) \tag{45}$$

where the mean $\tau_0 = \langle \tau \rangle$ is kept constant in this limit and the variance is vanishing. This limit is easily seen in the Laplace space

$$\lim_{\xi\to\infty} \hat{K}_{\xi,\xi\tau_0}(\tau) = \lim_{\xi\to\infty} \left(1 + \frac{\lambda}{\xi}\right)^{-\xi\tau_0} = e^{-\tau_0\lambda} = \int_0^\infty e^{-\lambda t} \delta(t - \tau_0) \mathrm{d}t. \tag{46}$$

4.2 Validation of the macroscopic SCIRS model and case study

In the simulations we remove unimportant fluctuations by recording the ensemble averaged[3] compartment populations $\langle s(t) \rangle, \langle c(t) \rangle, \langle r(t) \rangle, \langle j(t) \rangle$. We average numerically over a number of equivalent random walk realizations with identical parameters, waiting time distributions and observation times. Each realization employs different random numbers ('python seeds') for the waiting times and random walk. We perform a case study to validate the macroscopic

[3]We denote here ensemble averages of random functions $B(t)$ with $\langle B(t) \rangle$.

Eqs. (28) for the endemic equilibrium which exists for $R_0 = \beta t_I > 1$. We realize 'natural' initial conditions close to the healthy state with one infected walker (in compartment I) and $Z-1$ susceptible walkers at $t = 0$ (start of the experiment). In all computer experiments the walkers have random initial positions on the lattice. We determine the endemic equilibrium values numerically by using the asymptotic relation

$$[S_e, C_e, J_e, R_e]_{num}(t) \approx \frac{1}{t}\sum_{r=1}^{t}\langle [s(r), c(t), j(t), r(t)]\rangle \tag{47}$$

converging for $t \to \infty$ to the endemic state S_e, C_e, J_e, R_e if it exists. We measure the accordance of our macroscopic endemic equations (28) with the random walk approach by computing the ratios of the numerically determined endemic values and the values computed with (28)

$$\begin{aligned} r_C &= \frac{(S_e)_{num}}{[1-(S_e)_{num}]\langle t_C\rangle/\langle T\rangle} \\ r_I &= \frac{(J_e)_{num}}{[1-(S_e)_{num}]\langle t_I\rangle/\langle T\rangle} \\ r_R &= \frac{(R_e)_{num}}{[1-(S_e)_{num}]\langle t_R\rangle/\langle T\rangle} \end{aligned} \tag{48}$$

by employing the numerically determined S_e. In all simulations with existing endemic equilibria and sufficiently large observation time the ratios $r_{C,I,R} \approx 1 + O(10^{-2})$ are up to a few percent close to one, confirming impressively the prediction $C_e : J_e : R_e = \langle t_C\rangle : \langle t_I\rangle : \langle t_I\rangle$ of the macroscopic model Eqs. (28). In the following discussion we give numerical evidence that our macroscopic SCIRS model well suits with the microscopic random walk approach.

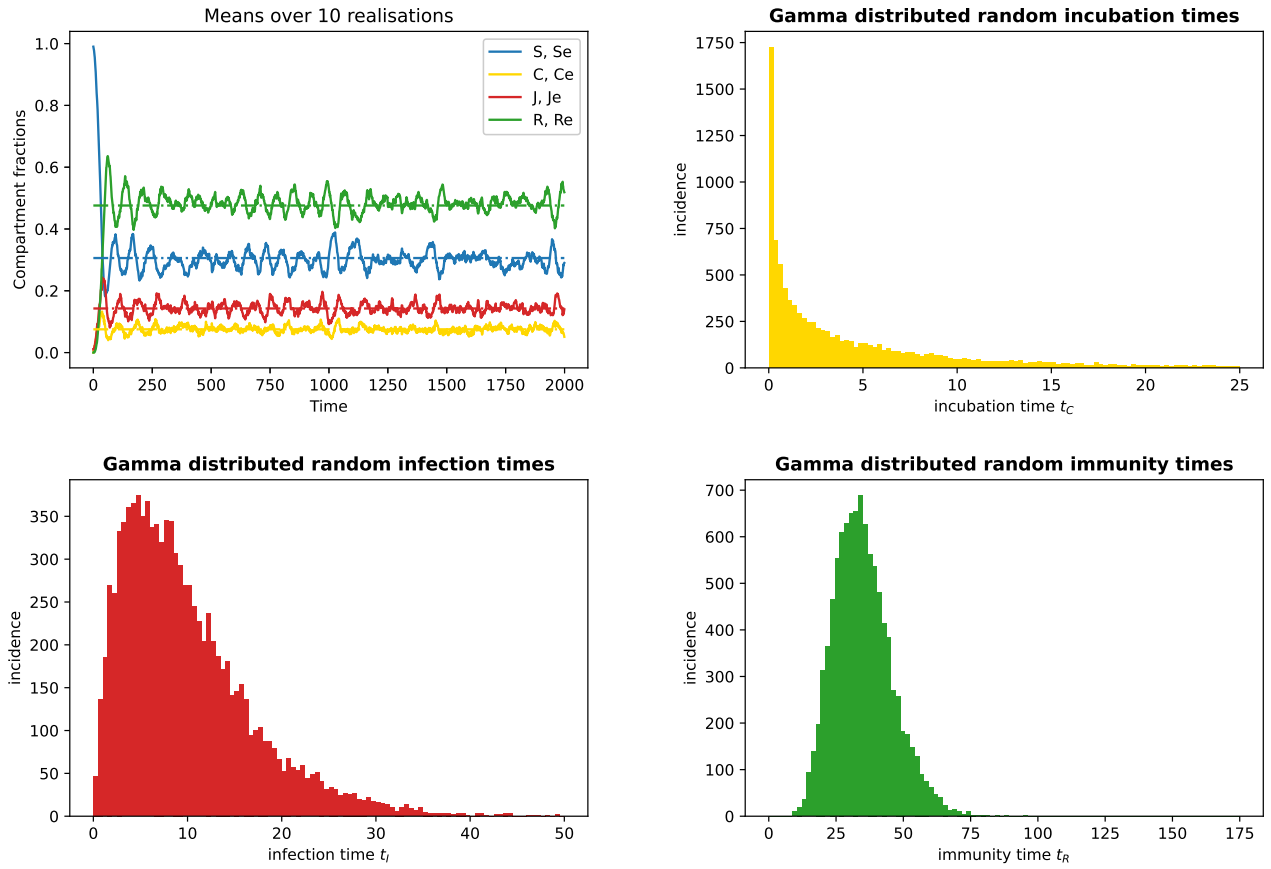

Figure 4: Average population fractions over 10 random walk realizations with $Z = 100$, $N = 11$ (density $Z/N^2 \approx 0.83$), $P_{inf} = 0.9$ and Gamma distributed waiting times having the means $\langle t_C\rangle = 5$, $\langle t_I\rangle = 10$, $\langle t_R\rangle = 35$, $\xi_C = 0.1$, $\xi_I = 0.2$, $\xi_R = 0.3$. By using Eq. (47) for the numerical evaluation we get (dashed lines) $S_e \approx 0.31$, $C_e \approx 0.075$, $J_e \approx 0.14$, $R_e \approx 0.48$ and with Eq. (48) we have $r_C \approx 1.08$, $r_I \approx 1.03$, $r_R \approx 0.98$. We depict the corresponding Gamma distributed waiting times $t_{C,I,R}$ in three histograms with the parameters used in this simulation.

In the experiment of Figure 4 the waiting times are broadly scattered and distributed by Gamma distributions of different parameters. For the chosen parameters the epidemic dynamics

converges rapidly to the endemic states where the ratio $C_e : J_e : R_e = \langle t_C \rangle : \langle t_I \rangle : \langle t_I \rangle$ predicted by Eqs. (28).

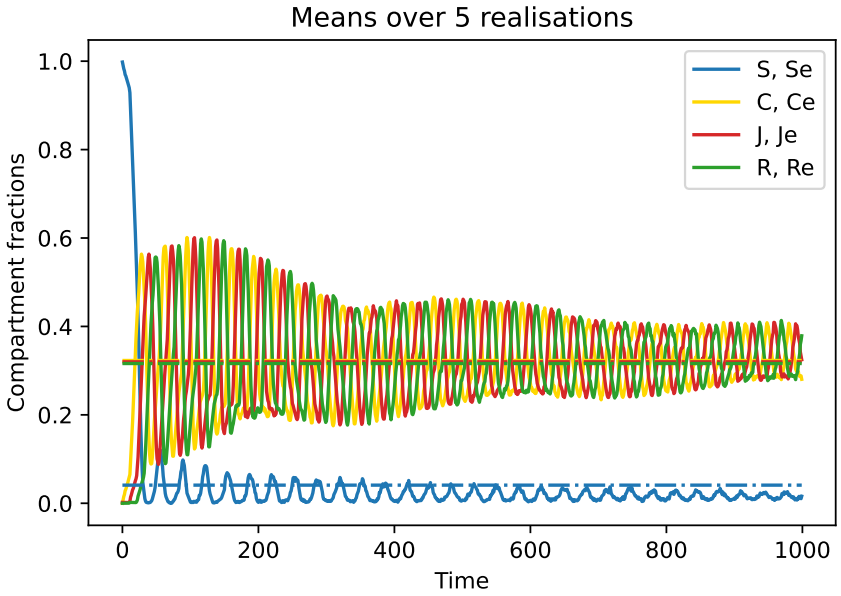

Figure 5: (a) Average over 5 random walk realizations and (δ-distributed) waiting times $t_C = t_I = t_R = 10$ ($T = 30$) with $Z = 500$, $N = 11$ (density $Z/N^2 \approx 4.13$), $P_{inf} = 0.9$. We have small $S_e \approx 0.04$ ($R_0 \approx 24, 39$) and $C_e = J_e = R_e \approx 0.32 \approx \frac{1}{3}$ (dashed lines).

In Figure 5 we have equal δ-distributed waiting times and very large R_0. The measures (48) are $r_{C,I,R} \approx (1, 01, 1, 0.99)$ close to one and indicate excellent accordance with Eqs. (28) although the observation time is not very large. In this plot (blue dashed line) S_e is slightly overestimated as (47) is an asymptotic relation holding for large t.

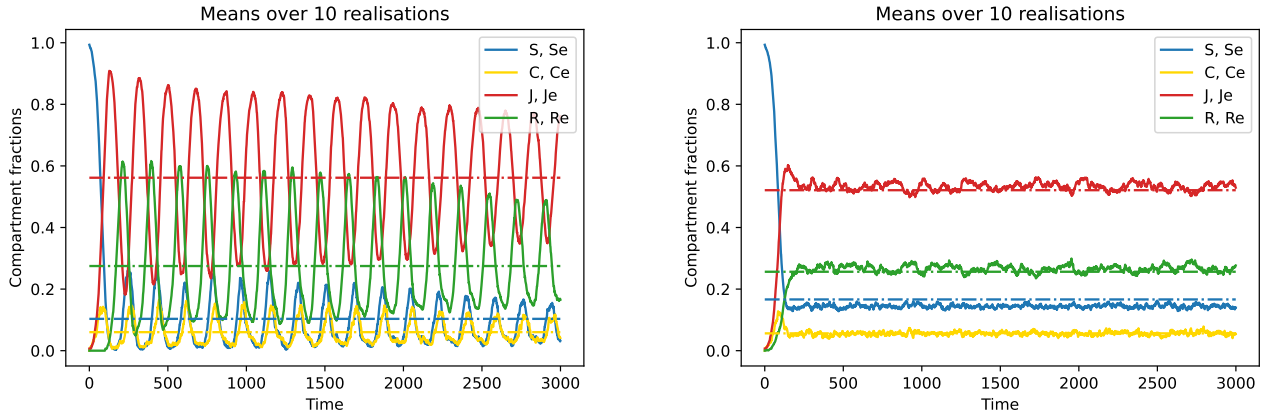

Figure 6: δ-distributed (frame on the left) and exponentially distributed waiting times (frame on the right) with $Z = 150$, $N = 21$ (density $Z/N^2 \approx 0.34$), $P_{inf} = 0.9$, mean incubation time $\langle t_C \rangle = 10$, $\langle t_I \rangle = 100$, $\langle t_R \rangle = 50$.
Endemic state (δ-distributed waiting times, dashed lines figure on the left): $S_e \approx 0.10$ ($R_0 \approx 9.68$), $C_e \approx 0.06$, $J_e \approx 0.56$, $R_e \approx 0.27$,
$r_C \approx 0.07$, $r_I \approx 1.00$, $r_R = 0.98$.
Endemic state (exponential waiting times, dashed lines figure on the right): $S_e \approx 0.16$ ($R_0 \approx 6.01$), $C_e \approx 0.06$, $J_e \approx 0.52$, $R_e \approx 0.26$
$r_C \approx 1.07$, $r_I \approx 1.00$, $r_R \approx 0.98$

The depicted time evolutions of Figures 6 exhibit for δ-distributed waiting times slightly attenuated oscillations. This indicates that this case is close to an oscillatory (Hopf-) instability.

We approach this instability by slightly reducing the walkers density (reducing R_0). The corresponding persistent oscillatory behavior is shown in the left frame of Figure 7.

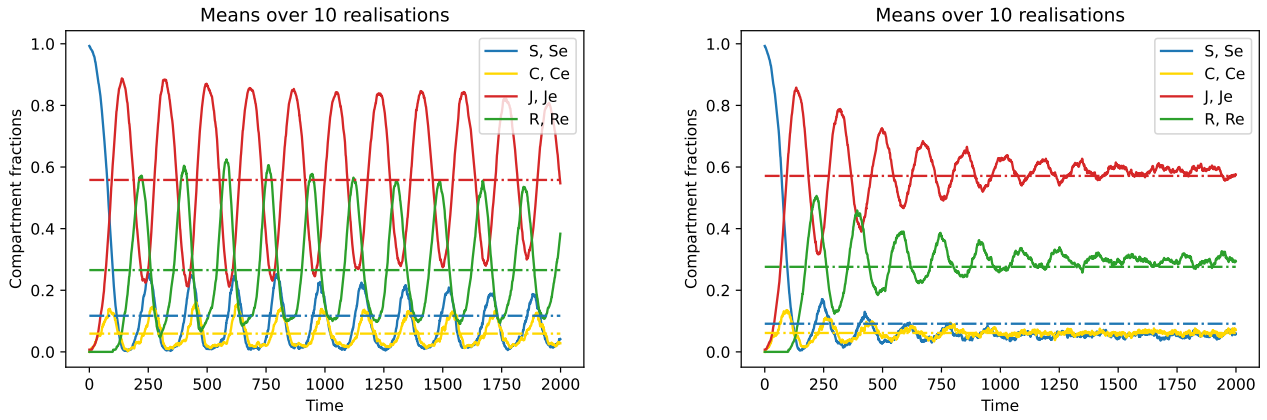

Figure 7: *Left frame:* δ-distributed waiting times, all parameters as in the left frame of Figure 6 but with $Z = 140$ to have a slightly lower density to approach the oscillatory (Hopf) instability (density $Z/N^2 \approx 0.32$). Endemic values: $S_e \approx 0.11$ ($R_0 \approx 9.09$), $C_e \approx 0.06$, $J_e \approx 0.56$, $R_e \approx 0.26$ $r_C \approx 1.07$, $r_I \approx 1.01$, $r_R \approx 0.96$.
Right frame: Identical parameters (including density) as for the left frame but with exponentially distributed t_C (with $\langle t_C \rangle = 10$), Gamma-distributed t_R with $\xi_R = 0.1$ and $\langle t_R \rangle = 50$ and t_I is δ-distributed ($t_I = 100$). The different types of distributions decrease slightly $S_e \approx 0.09$ with increasing $R_0 \approx 10.95$ compared to the left frame leading to attenuated oscillations. Other endemic values $C_e \approx 0.06$, $J_e \approx 0.57$, $R_e \approx 0.28$,
$r_C \approx 1.08$, $r_I \approx 1.00$, $r_R \approx 0.97$

Both plots in Figure 7 differ by changing to exponentially distributed t_C, and Gamma distributed t_R. All other parameters including the density are identical in both frames. The left frame exhibits an Hopf unstable persistent oscillatory behavior. The resulting S_e of the right frame is slightly lower increasing R_0 and leading to attenuation of the Hopf oscillations. This demonstrates as both plots employ identical parameters but different waiting time PDFs that R_0 also depends on further characteristics such as for instance the variance.

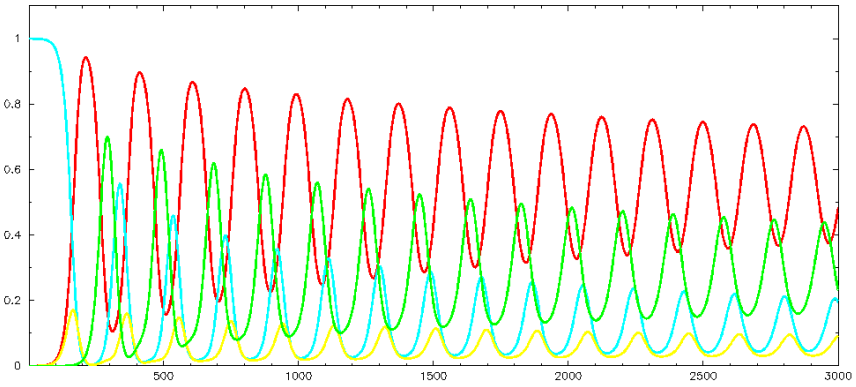

Figure 8: Numerical solution of the ODE model (30) with the parameters of Figure 7 (left frame) and $R_0 = 9.1$, $j_0 = 0.01$, $s_0 = 0.99$, $c_0 = r_0 = 0$. The color code is the same as in Figure 7.

The plot in Figure 8 shows a numerical solution of the macroscopic system (30) for the same parameters as in (frames on the left) of Figures 6 and 7. The at least qualitative similarity to the microscopic result is impressive (see especially left frame of Figure 6 exhibiting attenuated oscillations). In both models the number of infectious dominates due to the relatively long

infection time. In the long time limit the oscillations are damped and the endemic equilibrium is asymptotically reached.

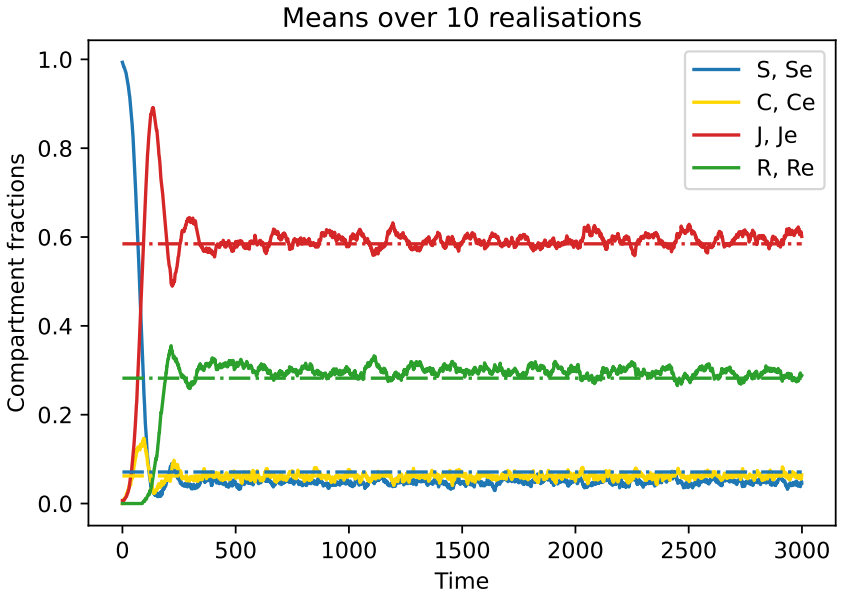

Figure 9: Gamma distributed waiting times. Same parameters as in Figure 6 except $\xi_C = 0.5$, $\xi_I = 0.2$, $\xi_R = 0.01$,
Endemic state (dashed lines): $S_e \approx 0.07$ ($R_0 \approx 14.09$), $C_e \approx 0.06$, $J_e \approx 0.58$, $R_e \approx 0.28$
$r_C \approx 1.06$, $r_I \approx 1.00$, $R_R \approx 0.97$.

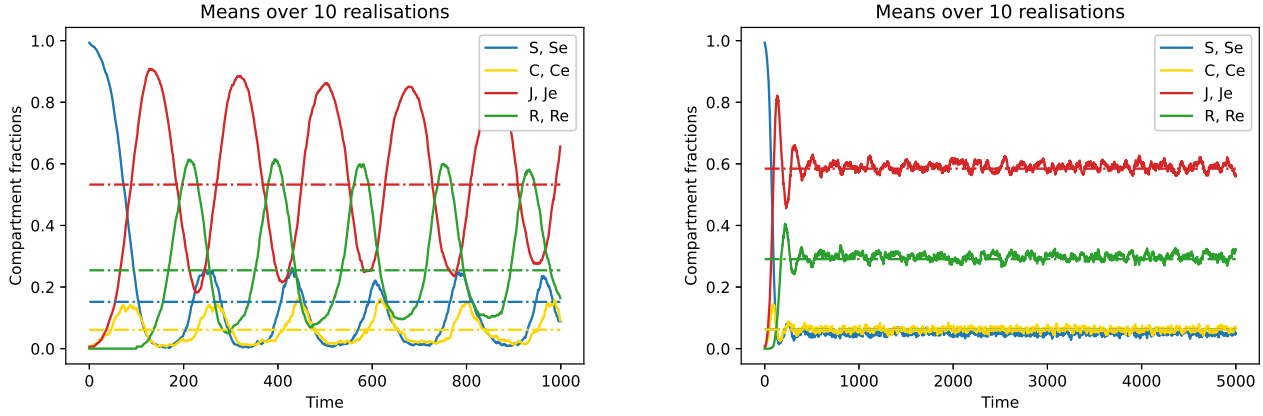

Figure 10: *Left frame*: δ-distributed waiting times all parameters are identical as in the right frame, except $\xi_{C,I,R} = 10^4$ (generating the δ-distribution, see (45)). Endemic values (dashed lines): $S_e \approx 0.15 (R_0 = 1/S_e \approx 6.59), C_e \approx 0.6, J_e \approx 0.53, R_e \approx 0.25$.
$r_C \approx 1.15$, $r_I \approx 1.00$, $r_R \approx 0.96$.
Right frame: All waiting times are Gamma distributed where their means are identical with those of the left frame with $\langle t_C \rangle = 10$, $\xi_C = 0.1$, $\langle t_I \rangle = 100$, $\xi_I = 0.1$ ($\alpha_I = 10$), $\langle t_R \rangle = 50$, $\xi_R = 0.05$, $Z = 150$, $N = 21$ (density $Z/N^2 \approx 0.34$), $P_{inf} = 0.9$,
$S_e \approx 0.06 (R_0 = 1/S_e \approx 15.91), C_e \approx 0.06, J_e \approx 0.58, R_e \approx 0.29$,
$r_C \approx 1.06$, $r_I \approx 0.99$, $r_R \approx 0.99$.

In the simulations of Figures 9 and 10 we consider various combinations of waiting time distributions. In Figure 10 we compare δ-distributed waiting times and Gamma distributed waiting times with the same means. In the left frame r_C has with 15% a relative large deviation from Eq. (28). This can be explained as as (47) is an asymptotic relation converging for large

t to the endemic values where in the left frame the time is not very large. In the right frame the time is increased thus all $r_{C,I,R}$ are very close to one indicating excellent accordance with Eq. (28). The slightly different absolute values are due to slightly different $R_0 = 1/S_e$ despite all parameters P_{inf}, Z, N are identical. This confirms our observation in Figures 7 that R_0 depends on further characteristics of the waiting time PDFs such as for instance their variances.

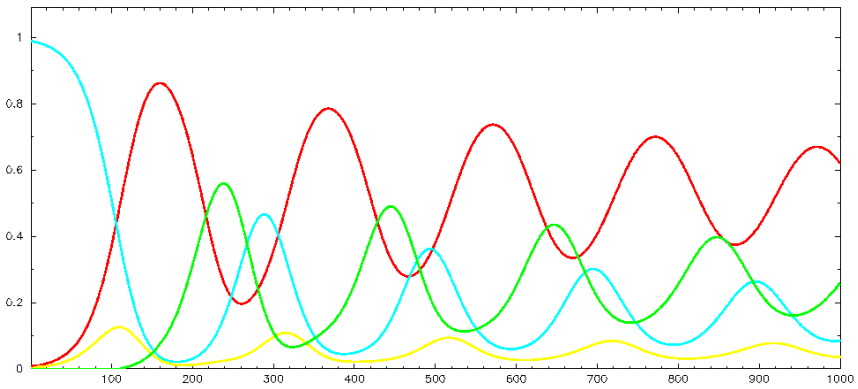

Figure 11: Numerical solution of the ODE model (30) with the parameters of Figure 10 (left) and $R_0 = 6.6,\ j_0 = 0.01,\ s_0 = 0.99,\ c_0 = r_0 = 0$.

Figure 11 shows again the numerical solution of the macroscopic system (30) which are here for the smaller R_0 again in good agreement with the averaged microscopic behavior.

5 Conclusions

We studied a macroscopic four compartment SCIRS model with memory effects introduced by random compartmental waiting times. We derived evolution equations for different arbitrary waiting time distributions and considered pertinent cases such as exponential (memoryless), Mittag Leffler (fat-tailed with long memory), and sharp (δ-distributed) waiting times. We highlighted connections with general fractional calculus and showed that the evolution equations are of general (fractional) type (Eqs. (11), (49)). For waiting time PDFs with existing mean we obtained exact formulas for the endemic equilibrium and conditions of its existence and identified the 'basic reproduction factor' $R_0 = \beta\langle t_I\rangle$ as crucial parameter controlling whether or not a SCIRS epidemic starts to spread.

We also found (Appendix B) that the healthy state always is unstable if t_I has a fat-tailed PDF regardless of the distributions of $t_{C,R}$. In this case R_0 and $\langle t_I\rangle$ do not exist. We interpret this instability by the occurrence of very long infectious periods t_I strongly boosting the epidemic spreading. Due to their general importance, the time-fractional cases call for further thorough investigations.

We compared the macroscopic SCIRS model with a random walk approach. Our computer experiments have given numerical evidence that Eqs. (28) are fulfilled for any of the implemented waiting time distributions (with initial conditions very close to the healthy state) whenever the endemic equilibrium exists. This is further confirmed by comparison of results produced by the random walk simulations and by direct numerical integration of Eqs. (30) for two cases of δ-distributed waiting times, see Figures 6 (left), 8 and 10 (left), 11, respectively. All these results give strong evidence that random walks offer an appropriate microscopic picture of the SCIRS dynamics. It is also found in the simulations that waiting time PDFs with different variances but otherwise identical parameters may influence R_0.

For future research it would be desirable to relate the endemic value S_e (i.e. R_0) (here determined numerically) with characteristics of the waiting time PDFs (such as their variances and others), infection probabilities in a collision of I and S walkers and of the random walk. A

further challenge is the development of a microscopic random walk model for the oscillatory (Hopf) instabilities (condition for persistent oscillatory behavior).

Generally SCIRS type models with memory as introduced in the present paper may open a wide research field to better understand the phenomenology of real world epidemic dynamics.

Acknowledgement

T.G. gratefully acknowledges to have been hosted at the Institut Jean le Rond d'Alembert for the sake of the present study and development of the Python codes.

A General derivatives

We can alternatively represent Eqs. (11) in the Riemann-Liouville sense of general derivatives as

$$\begin{aligned}
\frac{d}{dt}s(t) &= -\mathcal{A}(t) + \frac{d}{dt}\int_0^t \mathcal{L}_R(t-\tau)r(\tau)\mathrm{d}\tau \\
\frac{d}{dt}c(t) &= \mathcal{A}(t) - \frac{d}{dt}\int_0^t \mathcal{L}_C(t-\tau)c(\tau)\mathrm{d}\tau \\
\frac{d}{dt}j(t) &= \frac{d}{dt}\int_0^t \mathcal{L}_C(t-\tau)c(\tau)\mathrm{d}\tau - \frac{d}{dt}\int_0^t \mathcal{L}_I(t-\tau)[j(\tau)-j_0]\mathrm{d}\tau \\
\frac{d}{dt}r(t) &= \frac{d}{dt}\int_0^t \mathcal{L}_I(t-\tau)[j(\tau)-j_0]\mathrm{d}\tau - \frac{d}{dt}\int_0^t \mathcal{L}_R(t-\tau)r(\tau)\mathrm{d}\tau
\end{aligned} \tag{49}$$

which also is obtained straight-forwardly from the Laplace transformed representation (9) and employing definition (10). On the right-hand sides general derivatives come into play. The notion of 'general' (fractional) derivative was introduced by Kochubei [29] generalizing $\frac{d}{dt}y(t)$ as (in the Caputo sense)

$$D_t^* \cdot y(t) = \int_0^t k(t-\tau)\frac{d}{d\tau}y(\tau)\mathrm{d}\tau = \frac{d}{dt}\int_0^t k(t-\tau)y(\tau)\mathrm{d}\tau - y_0 k(t) = D_t \cdot y(t) - y_0 k(t) \tag{50}$$

with $y_0 = y(t)\Big|_{t=0}$. The part $D_t \cdot y(t) = \int_0^t k(t-\tau)y(\tau)\mathrm{d}\tau$ is a general derivative in the Riemann-Liouville sense for some admissible kernels $k(\tau)$ (see [29] for an outline of this theory). The general derivative (50) has the LT

$$\int_0^\infty e^{-\lambda t} D_t y(t)\mathrm{d}t = \lambda\hat{k}(\lambda)\hat{y}(\lambda) - y_0\hat{k}(\lambda) \tag{51}$$

The general derivatives contain the class of standard fractional derivatives of Caputo and Riemann-Liouville type and for a $k(t) = \delta(t)$ the standard first order derivative.

B Stability analysis for arbitrary waiting time densities

In Section 3 we have derived that the healthy state is unstable if $R_0 = \beta t_I > 1$ for δ-distributed kernels. Here we consider arbitrary waiting time kernels first with finite means to generalize this result and at the end of this appendix we briefly look at the time fractional case. To this end we take into account that the PDFs $K_{C,I,R}(t)$ can be seen as a superposition (average over $t_{C,I,R}$) of the $\delta(t - t_{C,I,R})$-kernel as follows

$$K_{C,I,R}(t) = \langle\delta(t - t_{C,I,R})\rangle = \int_0^\infty \delta(t-\tau)K_{C,I,R}(\tau)\mathrm{d}\tau = (\delta \star K_{C,I,R})(t) \tag{52}$$

and in this way we can average

$$\langle f(t_{C,I,R})\rangle = \int_0^\infty K_{C,I,R}(\tau) f(\tau)\mathrm{d}\tau \tag{53}$$

for sufficiently good functions f thus

$$\langle e^{-\mu t_{C,I,R}}\rangle = \hat{K}_{C,I,R}(\mu) \tag{54}$$

yielding the Laplace transform of the PDF. Therefore, averaging Eqs. (30) for δ-kernels over the waiting times $t_{C,I,R}$ brings us back to the general SCIRS Eqs. (1) which can be seen from

$$\langle \mathcal{A}(t-t_C)\rangle = \int_0^t \mathcal{A}(t-\tau)K_c(\tau)\mathrm{d}\tau = (K_C \star \mathcal{A})(t) \tag{55}$$

where we used causality of $\mathcal{A}$ and K_C. Hence we can generalize the case of δ-kernels (34) to any kernels by accounting for

$$\langle e^{-\mu(t_I+t_R+t_C)}\rangle = \hat{K}_C(\mu)\hat{K}_I(\mu)\hat{K}_R(\mu)$$

where we always use the mutually independence of the waiting times. Hence by averaging Eq. (34) we get

$$\begin{aligned} A_0(u,w)[1-\hat{K}_C(\mu)\hat{K}_I(\mu)\hat{K}_R(\mu))] + \mu u &= 0 \\ A_0(u,w)[1-\hat{K}_C(\mu)] - \mu v &= 0 \\ A_0(u,w)\hat{K}_C(\mu)[1-\hat{K}_I(\mu)] - \mu w &= 0 \\ A_0(u,w)\hat{K}_C(\mu)\hat{K}_I(\mu)[1-\hat{K}_R(\mu)] - x\mu &= 0 \end{aligned} \tag{56}$$

leading to the solvability condition

$$\left\| \begin{array}{cc} \beta J_e[1-\hat{K}_C(\mu)\hat{K}_I(\mu)\hat{K}_R(\mu)] + \mu; & \beta S_e[1-\hat{K}_C(\mu)\hat{K}_I(\mu)\hat{K}_R(\mu)] \\ \beta J_e\hat{K}_C(\mu)[1-\hat{K}_I(\mu)]; & \beta S_e\hat{K}_C(\mu)[1-\hat{K}_I(\mu)] - \mu \end{array} \right\| \mu^2 = 0. \tag{57}$$

We have again (as in (35)) $\mu = 0$ as a threefold eigenvalue. The remaining non-zero eigenvalue is determined by

$$\mu = \beta S_e\hat{K}_C(\mu)[1-\hat{K}_I(\mu)] - \beta J_e[1-\hat{K}_C(\mu)\hat{K}_I(\mu)\hat{K}_R(\mu)] \tag{58}$$

We have to point out that in order to obtain these results we have relaxed causality in the exponential ansatz (33) and assumed that it is defined for all $t \in \mathbb{R}$. The difference of causal and non-causal averaging can be seen by comparing

$$\begin{aligned} \left\langle e^{\mu(t-t_C)}\right\rangle = \;& e^{\mu t}\int_0^\infty e^{-\mu\tau}K_C(\tau)\mathrm{d}\tau = \hat{K}_C(\mu) \\ & \neq \left\langle \Theta(t-t_C)e^{\mu(t-t_C)}\right\rangle = e^{\mu t}\int_0^t e^{-\mu\tau}K_C(\tau)\mathrm{d}\tau \end{aligned} \tag{59}$$

where $\Theta(\tau)$ indicates the Heaviside unit step function and corresponds to causality. To obtain the condition (57) we have averaged as in the first line of (59) where the exponential is non-causal allowing exponentials with arguments $t-t_C < 0$ to contribute. Both sides become asymptotically equal in the limit $t \to \infty$. Hence above relation (57) can also be interpreted as the large time asymptotics of causal averaging.

Let us focus now on the stability of the healthy state $s_0 = 1$. Then (58) yields ($S_e \to s_0 = 1$, $J_e \to j_0 = 0$)

$$\mu = \beta\hat{K}_C(\mu)[1-\hat{K}_I(\mu)] = G(\mu). \tag{60}$$

As in the case of δ-distributed waiting times $G(\mu)$ is a concave function with $G(\mu) \to 0$ as $\mu \to \infty$ thus we can argue in the same way (see Eq. (37) and Figure 2). Hence there is an intersection $\mu_0 > 0$ only if $\frac{d}{d\mu} G(\mu)\Big|_{\mu=0} > 1$. Expanding $G(\mu)$ (assuming existing mean $\langle t_I \rangle$) gives

$$G(\mu) = \beta[1 - \langle t_C \rangle \mu + o(\mu)]\langle t_I \rangle \mu = \beta \langle t_I \rangle \mu + o(\mu). \tag{61}$$

Therefore,

$$\frac{d}{d\mu} G(\mu)\Big|_{\mu=0} =: R_0 = \beta \langle t_I \rangle > 1 \tag{62}$$

is the condition for this instability of the healthy state and hence the interpretation as 'basic reproduction factor' R_0 makes sense. This holds for waiting time PDFs with existing means. On the other hand relation (60) holds for any waiting time PDF including fat-tailed ones which we briefly consider in the following.

Time fractional case

Assuming $K_I(t)$ is a fat-tailed PDF such as Mittag-Leffler with $\hat{K}_I(\mu) = \frac{\xi_I}{\xi_I + \mu^\nu}$, $\nu \in (0, 1)$ and no matter whether or not the other kernels have existing means we get for $G(\mu)$

$$G(\mu) = \frac{\beta}{\xi_I} \mu^\nu + o(\mu^\nu) > \mu \qquad\qquad (\mu \to 0) \tag{63}$$

where $o(\mu^\nu)$ indicates orders higher than ν. Thus (60) (independent of $\frac{\beta}{\xi_I}$) always has a positive intersection since $\nu \in (0, 1)$. *We conclude that for fat-tailed $K_I(t)$ the healthy state always is unstable regardless of the distributions of t_C and t_R.* Physically this instability can be understood by the occurrence of very long infectious times t_I strongly boosting the epidemic spreading (corresponding to the limit $R_0, \langle t_I \rangle \to \infty$).

References

[1] W.O. Kermack, A.G. McKendrick, A contribution to the mathematical theory of epidemics, Proc. Roy. Soc. A 115, 700–721 (1927)

[2] R. M. Anderson, and R. M. May, 1992, Infectious Diseases in Humans, (Oxford University Press, Oxford).

[3] M. Martcheva, An Introduction to Mathematical Epidemiology, Springer (2015)

[4] V. Belik, T. Geisel, D. Brockmann, 'Recurrent host mobility in spatial epidemics: beyond reaction-diffusion', Eur. Phys. J. B 84, 579-587 (2011)

[5] L. Feng, Q. Zhao, C. Zhou, 'Epidemic spreading in heterogeneous networks with recurrent mobility patterns', Phys. Rev. E 102, 022306 (2020)

[6] A.–L. Barabási, Network science (Cambridge University Press, Cambridge, 2016).

[7] R. Pastor-Satorras, A. Vespignani 'Epidemic dynamics and endemic states in complex networks', Phys. Rev. E 63, 066117 (2001)

[8] A.P. Riascos, J.L. Mateos, 'Random walks on weighted networks: a survey of local and non-local dynamics', J. Complex Networks 9, cnab032 (2021)

[9] T. Michelitsch, A. P. Riascos, B. A. Collet, A. Nowakowski, F. Nicolleau, Fractional Dynamics on Networks and Lattices, ISTE-Wiley, London, (2019). ISBN : 9781786301581.

[10] M. Bestehorn, A.P. Riascos, T. M. Michelitsch, B.A. Collet, 'A Markovian random walk model of epidemic spreading', Continuum Mech. Thermodyn. 33, 1207 (2021)

[11] M. Bestehorn, T.M. Michelitsch, B.A. Collet, A.P. Riascos, A.F. Nowakowski, 'Simple model of epidemic dynamics with memory effects, Phys. Rev. E 105, 024205 (2022)

[12] R. Metzler, J. Klafter, 'The Random Walk's Guide to Anomalous Diffusion : A Fractional Dynamics Approach', Phys. Rep. 339, 1-77 (2000)

[13] T. Sandev, R. Metzler, A. Chechkin, 'From Continuous Time Random Walks to the Generalized Diffusion Equation', Fract. Calc. Appl. Anal. 21, 10-28 (2018).

[14] F. Mainardi, R. Gorenflo, E. Scalas, A fractional generalization of the Poisson processes, Vietnam J. Math. 32 (2004) 53–64, MR2120631.

[15] T.M. Michelitsch, F. Polito, A.P. Riascos, Biased Continuous-Time Random Walks with Mittag-Leffler Jumps, Fractal Fract. 4, 51 (2020) doi:10.3390/fractalfract4040051

[16] T.M. Michelitsch, A.P. Riascos, Generalized fractional Poisson process and related stochastic dynamics, Fract. Calc. Appl. Anal., Vol. 23, No 3 (2020), pp. 656–693, DOI: 10.1515/fca-2020-0034

[17] H.E. Soper, 'The interpretation of periodicity in disease prevalence', J. R. Stat. Soc. 92, 34 (1929)

[18] H. C. Tijms (18 April 2003). A First Course in Stochastic Models. John Wiley & Sons, ISBN 978-0-471-49880-3.

[19] A.J. Lotka, Analytical Theory of Biological Populations, Plenum Press New York (1998)

[20] F.A. Rihan, Delay Differential Equations and Applications to Biology, Springer Nature Singapure (2021)

[21] G.E. Hutchinson, Circular causal systems in ecology, N.Y. Acd. Sci. 50 221 (1948)

[22] D. Mackey, L. Glass, Oscillations and chaos in physiological control systems, Science 197, 28 (1977)

[23] M. Bestehorn, E.V. Grigorieva, S.A. Kaschenko, Spatio-temporal structures in a model with delay and diffusion, Phys. Rev. E 70, 026202 (2004)

[24] L. Basnarkov, I. Tomovski T. Sandev, L. Kocarev, 'Non-Markovian SIR epidemic spreading model', arXiv:2107.07427 (2021)

[25] M. Bestehorn, Computational Physics, De Gruyter Berlin/Boston (2018)

[26] T.M. Michelitsch, F. Polito, A.P. Riascos, On discrete time Prabhakar-generalized fractional Poisson processes and related stochastic dynamics, Physica A 565 (2021) 125541

[27] W. Feller, An Introduction to Probability and Its Applications, vol. 1, 3rd edition, New York: Wiley, (1968)

[28] S.G. Samko, A.A. Kilbas, O.I. Marichev, Fractional Integrals and Derivatives: Theory and Applications, Gordon and Breach, London, 1993.

[29] Kochubei, A.N. General fractional calculus, evolution equations, and renewal processes. Integral Equ. Oper. Theory 2011, 71, 583–600

[30] See (Web link to be included) – Code Python © Téo Granger 2022.